Chinese Chemical Letters 33 (2022) 3873–3878

Contents lists available at ScienceDirect

Chinese Chemical Letters

journal homepage: www.elsevier.com/locate/cclet

Engineering a cationic supramolecular charge switch for facile amino acids enantiodiscrimination based on extended-gate field effect transistors

Jing-Jing Zhang[a], Si-Ying Wang[a], Pan Zhang[a], Shu-Chen Fan[a], Hai-Tao Dai[b], Yin Xiao[c,*], Yong Wang[a,*]

[a] School of Science, Tianjin Key Laboratory of Molecular Optoelectronic Science, Department of Chemistry, Collaborative Innovation Center of Chemical Science and Engineering, Tianjin University, Tianjin 300072, China
[b] Tianjin Key Laboratory of Low Dimensional Materials, Physics and Preparing Technology, Department of Physics, School of Science, Tianjin 300072, China
[c] School of Chemical Engineering and Technology, Tianjin Engineering Research Center of Functional Fine Chemicals, Tianjin University, Tianjin 300072, China

ARTICLE INFO

Article history:
Received 13 September 2021
Revised 26 October 2021
Accepted 25 November 2021
Available online 2 December 2021

Keywords:
Enantiodiscrimination
EG-OFET
Cyclodextrins
Chirality amplification
Amino acids

ABSTRACT

Chiral recognition of essential amino acids (EAAs) is a huge challenge that keeps plaguing analytical scientists due to their cryptochirality and limited steric interaction sites. Inspired by the superior enantioselectivity of functional supramolecular cyclodextrins (CDs) and strong signal amplification ability of field effect transistors (FETs), this work firstly reports a cationic supramolecular charge switch for facile enantiodiscrimination of EAAs based on extended-gate organic FET (EG-OFET). The cationic phenylcarbamoylated-CD single isomer acts as a charge switch *via* interacting with different enantiomers and the weak stereo-differentiation intermolecular interaction signals between the cationic perphenylcarbamoylated CDs and EAAs on the EG can be strongly and rapidly amplified through an OFET. Efficient chiral differentiation of six EAAs, including phenylalanine, tryptophan, leucine, isoleucine, lysine and valine, are successfully achieved without any derivation process and the detection limit for D-phenylalanine is down to 10^{-13} mol/L. We believe that this study provides a new and facile sensing perspective for natural amino acids and may afford deeper understanding of molecular chirality.

Chirality is one of the ubiquitous and hard-wired attributes of nature [1]. As the basic unit of living organism, amino acids (AAs) exhibit chiral properties and build the complex vivo chiral environment. Given different biological and toxicological effects that enantiomers may exhibit on living systems, enantiomers discrimination has attracted tremendous attention in the past few decades [2–4]. The chirality distributions of AAs may exhibit a unique pattern in living system [5,6], yet abiotic reactions generate a racemic mixture of AAs [7,8], which makes chiral distribution an important biosignatures to the emergence of biochemistry on planets.

Consequently, miscellaneous techniques have been established for recognition and separation of AAs [9,10]. However, most of those developed methods are not that efficient for AAs discrimination due to their cryptochirality and limited steric interaction sites [11]. For example, chiral AAs lack of chromophores cannot be detected by the powerful circular dichroism spectrogram [12,13]. In chromatography, derivation is usually needful not only for constructing compulsory differential interactions improving recognition but also to surmount the detection limitation [14–16]. Although electrochemical chiral sensing approaches have been applied for AAs chiral detection [17–22], they still suffer from complicated selector immobilization approaches and low sensitivity limited by concentration requirement of redox reactions. Thus, pursuing facile, effective and versatile sensing methods for AAs chiral discrimination is still a huge challenge for analytical scientists by far.

Organic field effect transistors (OFETs), as an ideal sensing platform *via* amplification of subtle change charge signals, have been increasingly investigated in various sensing fields owing to their fast response, compact integration and cost effectiveness [23,24]. Very recently, Sun *et al.* constructed an OFET chiral sensor with chemical-vapor-deposited (CVD) copper hexadeca-fluorine-phthalocyanine semiconductive layer using assembled β-cyclodextrin (β-CD) as sensing units for Phe-chiral detection [25]. Thereafter, Wu et al. used a similar quasi-gated OFET framework with a cationic β-CD sensing units to achieve

* Corresponding authors.
E-mail addresses: xiaoyin@tju.edu.cn (Y. Xiao), wangyongtju@tju.edu.cn (Y. Wang).

https://doi.org/10.1016/j.cclet.2021.11.081
1001-8417/

enantiodiscrimination at extremely low concentrations [26,27]. These works reveal the great potential of OFETs in chiral recognition and provide inspirations to develop reliable AAs enantiodiscrimination methodologies.

Inspired by the superior enantioselectivity of supramolecular CD and strong signal amplification ability of OFET, herein, we report a versatile, rapid and facile chirality amplification methodology for efficient enantiodifferentiation of essential AAs (EAAs) based on an extended-gate OFET (EG-OFET). Subtle difference of weak chiral interactions between p-tolyl isocyanate functionalized imidazolium β-CD (Im^+-MePh-β-CD) and EAAs pure optical enantiomers can be transferred to OFET. The cationic imidazolium moiety anchored on CD primary rim acts as a charge "switch" to modulate the effective gate bias of the OFET *via* alteration of the charge shielding effect. The switch is in an off-state when included in the extended CD cavity, while generating CDs-chiral analytes inclusion complexes will turn the switch on in varying degrees. Six EAAs enantiomers can be well differentiated without sample pretreatment with the detection limit down to 10^{-13} mol/L for D-phenylalanine (D-Phe).

To achieve the chirality signal amplification *via* EG-OFET, the premise is to construct enantio–selective interactions between the selector and chiral analytes. Synthesis of CD derivatives was referred to the published work [27,28]. CDs, as one of the most commonly used chiral selectors, were chosen for differentiation of EAAs in this work. Because of its poor enantioselectivity towards the underived EAAs, β-CD was decorated with twenty 4-methylphenylcarbamoyl and one imidazolium functionality, contributing strong electrostatic, π-π, dipole-dipole, H-bonding interactions and enhanced hydrophobic inclusion complexation (Figs. S1–S3 in Supporting information). Four optically pure EAAs (D-Phe, L-Phe, D-Lys and L-Lys) were chosen as model analytes to evaluate the intramolecular steric interactions with Im^+-MePh-β-CD by UV–vis, circular dichroism spectra, optical rotation analysis and 1 H NMR.

To get satisfied sensing layer on EG, the optimal Im^+-MePh-β-CD concentration was evaluated initially to be 10 mg/mL, according to membranes morphology (Fig. S4 in Supporting information). EG modification was proved by water contact angle measurement (Fig. S5 in Supporting information), which showed the reduced surface hydrophilicity after treatment with Im^+-MePh-β-CD. All the electrical tests were performed at room temperature. The output current of the OFET device was characterized under 50 V gate voltage (V_G) and 0–50 V drain-source (V_{DS}) voltage. The influence of matrix pH was also investigated (Fig. S6 in Supporting information). We initially investigated the intermolecular interactions using UV–vis (Fig. S7 in Supporting information). Im^+-MePh-β-CD exhibited strong absorption at *ca.* 201 nm and *ca.* 235 nm associated with π-π^* transition of double bonds. The B bands, characteristic absorption of aromatic rings, were observed at *ca.* 279 nm. After CD derivatives combining chiral AAs, there were no obvious bathochromic- or hypochromic-shift and the inclusion complexes only showed slightly-different adsorption intensity.

Interestingly, circular dichroism provided us some confident information about the chiral differentiation. Compared to native β-CD (no circular dichroism signal), strong positive (195 and 225 nm) and negative cotton peaks (207 and 240 nm) were observed with the well-defined Im^+-MePh-β-CD structure, revealing its intensive chiral conformation (Fig. 1a). Although the overall shape of circular dichroism curves for CD-AAs complexes only differed slightly compared to Im^+-MePh-β-CD, there were still distinct changes found between 190 and 200 nm with the emergence of low-intensity shoulder peaks (Figs. 1b and c) which might be attributed to the tiny conformation alteration of Im^+-MePh-β-CD arising from the weak interactions of AAs molecules with CD-CONH- moieties [29–31], since no circular dichroism signal was found with the optical pure EAAs at the same concentration (Fig. S8 in Supporting information). Excitingly, it was found that the peak intensity ratio (main peak/shoulder peak) for D- and L-Phe with CD was absolutely different (Fig. 1b), where the ratio for L-Phe (3.49) was much larger than D-Phe (1.55). Those results directly indicate the enantiodifferentiation ability of Im^+-MePh-β-CD toward Phe-enantiomers even if the steric interactions are not that strong. For Lys-enantiomers, however, this peak intensity ratio exhibited an opposite outcome (Fig. 1c), suggesting that Phe-and Lys-should experience different binding modes with Im^+-MePh-β-CD. The ratio value for D-Phe (1.55) was smaller than that of D-Lys (4.18) also suggesting the discrepant interaction types in each case. The phenyl group of Phe-could afford strong π-π stacking effect (lack in Lys) with the phenylcarbamoyl moieties, which might account for its larger alteration of such peak intensity ratio [32,33].

Thereafter, the optical rotation of Im^+-MePh-β-CD and its AAs complex were investigated (Fig. 1d). After binding with different chiral guests, the optical rotation of Im^+-MePh-β-CD was changed in different degrees while the pure AAs isomer with the same molar concentration could not cause obvious optical rotation, indicating the diverse binding conformation of the supramolecular complexes. As expected, D- and L-form AAs induced opposite optical rotation alteration of Im^+-MePh-β-CD. Besides, chain AAs Lys-caused the optical rotation of Im^+-MePh-β-CD in a gentler way than Phe-due to its lack of rigidity. It should be noted that L-P and D-Lys turned the optical rotation of Im^+-MePh-β-CD toward positive direction, which again verifies the different complex conformation formed between CD and the enantiomers and this is consistent with the conclusion drawn by the above circular dichroism results.

To make further investigation of the weak steric interactions between the cationic functional CD and EAAs enantiomers, the formation of the CD-AAs complex with 1:1 stoichiometry (molar ratio) was thereafter studied by ^{1}H NMR. The proton signals of Im^+-MePh-β-CD have been assigned according to reported values (Experiment section and Fig. S2) [34]. In the spectra range of CDs benzene rings, the signal intensity at 6.47 ppm reduced or vanishes when CD captured chiral molecules, yet nothing difference was found between enantiomers (Fig. S9 in Supporting information). Those changes could be attributed to the intermolecular π-π stacking and hydrophobic interactions between analytes and aromatic nucleus of phenyl carbamoyl substituents. The new peak at 5.76 ppm might also be attributed to the same reason. Based on the fact that the spectra change of Phe-CD complex was more obvious than Lys-CD, it is presumed that π-π stacking is stronger than hydrophobic force and plays a vital role in interacting with benzene rings. The spectra change founded in 1.82–1.91 ppm was exciting, which provides direct evidence that the intermolecular interactions are different for various EAAs enantiomers (Fig. 1e). The peak at 1.82 ppm showed different downfield shifts. Meanwhile, the peak area unchanged while the shape became sharper with the existence of optical isomers because the intermolecular interactions lengthened the relaxation time of the excited nuclei causing uncertainty shrinking at varying degrees [35]. Although the evidence of weak steric interactions between CDs derivatives and EAAs enantiomers has been found in ^{1}H NMR results, further investigation is still necessary to fully understand the enantioselectivity of Im^+-MePh-β-CD.

More specific information about the interaction mode between Im^+-MePh-β-CD and Phe-could be obtained from ROSEY spectra. Due to matched spatial configuration [36] and hydrophobic effect [37], Phe-trends to embed in the extended CD cavity consisted of phenyl carbamoyl substituents, which was also confirmed by the facts that no 2D signals were observed between Phe-and CDs cycloskeleton. Interestingly, the peak assigned to $-CH_3$ at 1.82 ppm showed downfield shifts (Fig. 1e), while it has no cross-peaks in

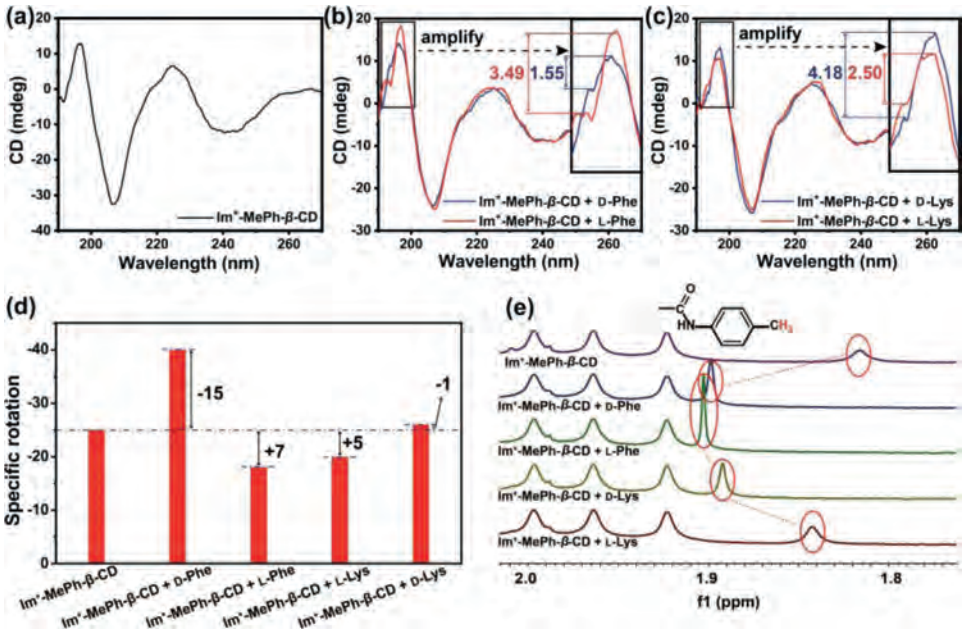

Fig. 1. Circular dichroism spectra of (a) Im$^+$-MePh-β-CD, (b) the complex of Phe-and Im$^+$-MePh-β-CD, and (c) the complex of Lys-and Im$^+$-MePh-β-CD. (d) Specific rotation of Im$^+$-MePh-β-CD as well as the 1:1 complex of Im$^+$-MePh-β-CD and AAs (Note: The specific rotation of pure AAs was not detectable at same concentrations). (e) ^{1}H NMR spectra of pure Im$^+$-MePh-β-CD and AAs-CD complexes.

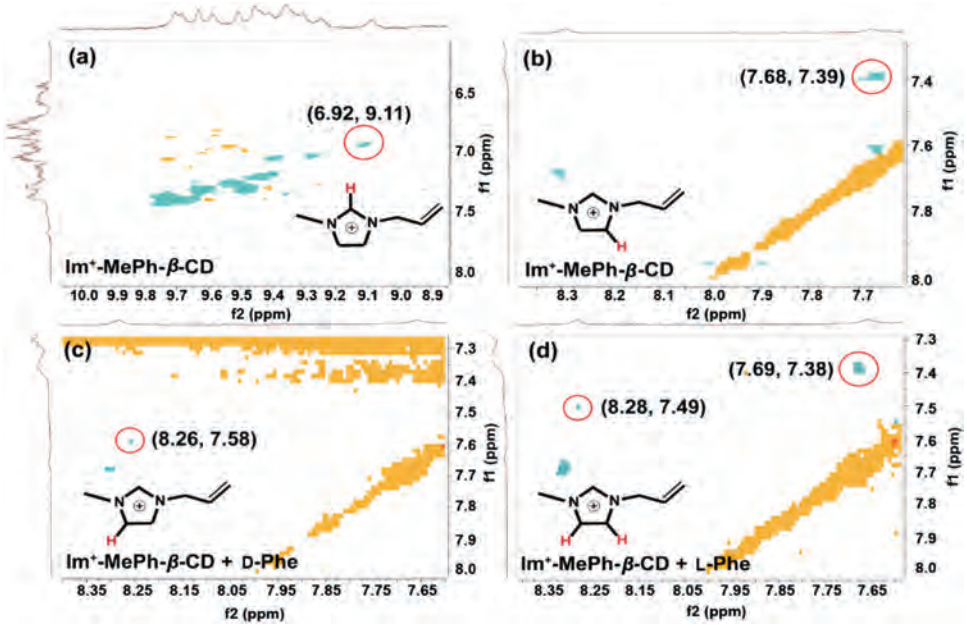

Fig. 2. ROSEY spectra of pure Im+-MePh-β-CD and Phe-CD complexes. (a) and (b) Im$^+$-MePh-β-CD imidazolium protons and benzene proton of phenyl carbamoyl, (c) and (d) Phe-CD imidazolium protons and benzene proton of phenyl carbamoyl.

ROSEY results (Fig. S10 in Supporting information). This indicates there exist intermolecular interactions between Phe-enantiomers and the CD phenyl carbamoyl moieties (actually the phenyl ring) which induces deshielded effect upon methyl proton. Meanwhile, the electron density reduction of benzenes resulted in a new signal at (1.9, 6.6) (Figs. S10b and c).

It was excited to find that the enantiomers combination could change the spatial relationship between cationic imidazolium moiety and extended cavity. Before Phe-is introduced, it is easy to conclude that the imidazolium is included in the extended cavity, based on cross-peaks between imidazolium protons and benzene proton of phenyl carbamoyl (Figs. 2a and b). The imidazolium positive charge is partially shielded by the surrounding electron cloud of phenyl carbamoyl substituents. However, after combining enantiomers, a new cross-peak could be detected (Figs. 2c and d), which is corresponded to the correlation between the cationic moiety and aromatic rings of Im$^+$-MePh-β-CD, and the original signal at (7.68, 7.39 ppm) disappeared in the spectra of CDs complexes with D-Phe guest.

Such results indicate that the imidazolium could be pushed out of the extended cavity ascribed to the combination with chiral isomers. Moreover, it should be noted that different combining modes are taken by Im$^+$-MePh-β-CD for Phe enantiomers. The cross-peaks between imidazolium and benzene rings vanished in

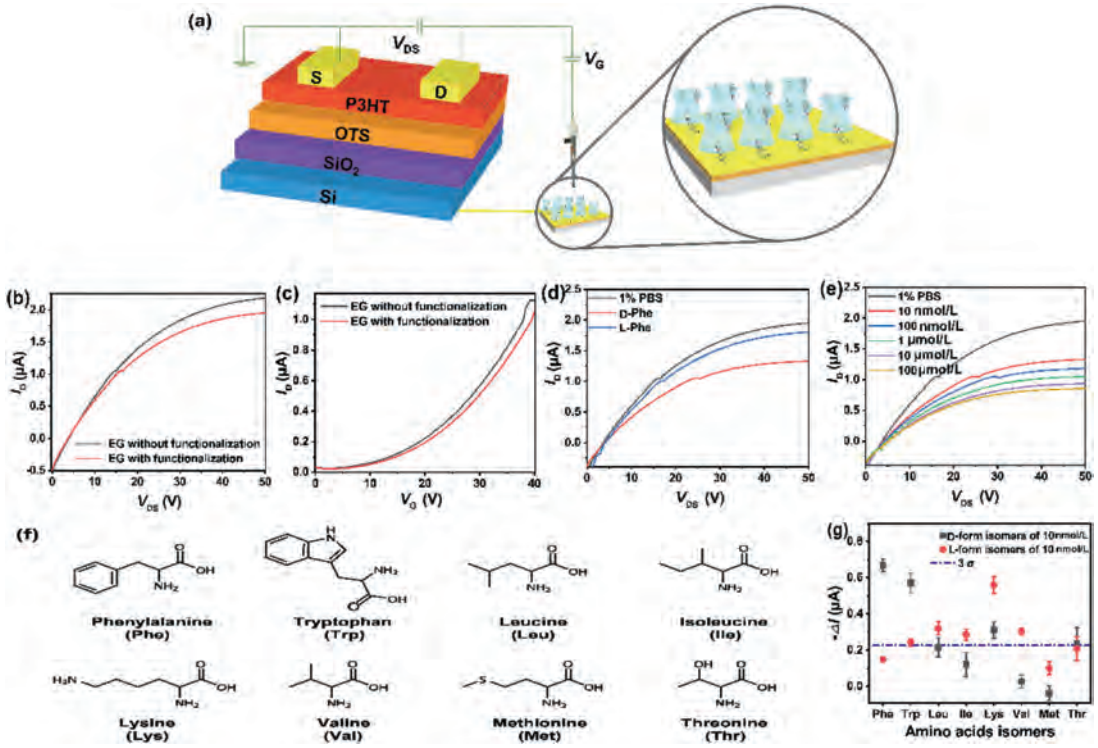

Fig. 3. (a) Schematic illustration of the EG-OFET architecture. (b) Output characteristic curves and (c) transfer characteristic curves of the fabricated sensing platform before and after Im^+-MePh-β-CD modification. (d) Chiral sensing responses and (e) concentration dependences of the EG-OFET upon detecting Phe. (f) Structures of the amino acids enantiomers. (g) Sensing responses toward various enantiomers with the concentration of 10 nmol/L in 1% PBS.

D-Phe complex but not L-form, indicating the higher degree of deshielding effects of cationic charge by D-Phe.

The above circular dichroism, optical rotation, ^{1}H NMR and ROSEY investigation results convince us the different enantioselective interacting modes between the selector and AAs enantiomers. Inspired by the subtle spatial variation of cationic imidazolium moiety, an EG-OFET chiral sensor was therefore developed based on this possible charging switch effect.

For the EG-OFET platform fabrication, Im^+-MePh-β-CD was employed as the sensing media to afford chiral resolution function. 4-methylphenylcarbamoyl substituents could help facilitate the film-forming ability *via* π-π stacking and hydrogen bonds formed between carbonyl and amino groups. According to the conclusion in previous section, the imidazolium moiety is expected to mediate gate voltage like a switch through altering electro positivity, transducing the host-guest distinct subtle interactions into the change of source and drain current (I_{DS}). The whole EG-OFET configuration was depicted in Fig. 3a.

The fabricated EG-OFET displayed typical p-channel behaviors, showing a field effect before and after Im^+-MePh-β-CD modification. The device could work normally and contain a stable electrical performance with mobility keeping at 0.006 $cm^2\ V^{-1}s^{-1}$, and only slight decreases in saturated drain current were observed. The representative I_{DS}-V_{DS} output and I_{DS}-V_G transfer characteristic curves were given in Fig. 3b and c. Upon detecting chiral AAs, output curves of different heights were given (Fig. 3d) and the current was decreased gradually with increasing solution concentration in the range of 10 nmol/L to 100 μmol/L (Fig. 3e).

Eight EAAs enantiomer pairs were used to evaluate the chiral amplification response of the established sensor (Fig. 3f). Fortunately, the output current of the device was found to be decreased upon AAs detection and different chiral configurations led to discrepant signal change (Fig. 3g), which revealed that enantiomers discrimination could be achieved successfully using the constructed EG-OFET. Interestingly and specifically, the signal caused by D-form was more obvious than L-form for Phe and Trp, while the opposite phenomenon happened to Lys, Leu-and Ile, which could be ascribed to different interaction models between EAAs and chiral selectors. For achieving good chiral sensing capacity of the fabricated system, the well-defined Im^+-MePh-β-CD was the key building block. Without Im^+-MePh-β-CD, EG-OFET hardly showed saturated drain current changes of AAs enantiomers. Both D- and L-AAs exhibited weak and similar current responses below the 3σ (σ: the standard deviation evaluated according to the response to blank for ten times) on bare gate resulting from their similar structures (Fig. S11 in Supporting information). Meanwhile, the capability of EG-OFET to amplify small interaction changes into electrical signals was also essential to realize chiral recognition. To guarantee the superior chiral recognition ability of the new sensing platform, Im^+-MePh-β-CD was immobilized onto thiol-silica with a 0.11 μmol/m^2 surface loading and employed as chiral stationary phase for enantioseparation of Phe and Trp enantiomers [34]. However, as shown in Fig. S12 (Supporting information), only single peak was obtained under various separation conditions indicating that the weak chiral interactions were not applicable for chromatography chiral separation and again affirmed the powerful amplification ability of such EG-OFET platform.

As shown in Fig. 4, concentration dependence was found with the sensing response, revealing the potentiality of the as-prepared EG-OFET for quantitative chiral analysis. The saturated drain current changes $\Delta I = (I - I_0)$ at $V_G = 50$ V for each pair of enantiomers were used to represent the sensing responses of the EG-OFET, where I_0 and I were the saturated drain currents before and after the addition of analytes, respectively. It should be noted that the as-prepared sensor afforded sensitive discrimination to the EAAs enantiomers with the limit of detection (LOD) as low as 10^{-13}, 10^{-11} and 10^{-12} mol/L for D-Phe, L-Lys and D-Trp, respectively, according to the line fitted results listed in Table S1

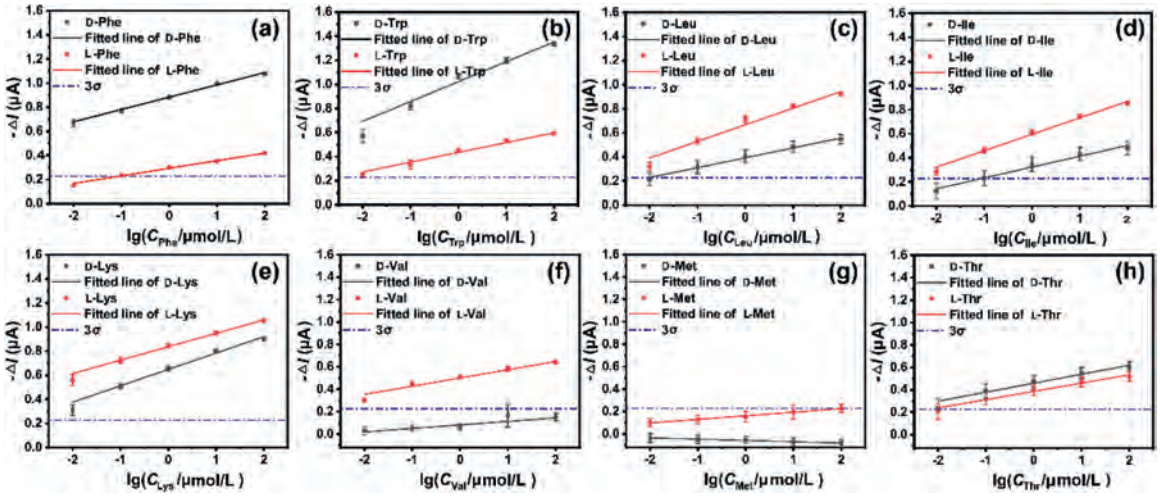

Fig. 4. The linear fitted chiral sensing responses of the EG-OFET upon detecting (a) Phe, (b) Trp, (c) Leu, (d) Ile, (e) Lys, (f) Val, (g) Met, and (h) Thr-enantiomers in 1% PBS solution.

(Supporting information). To further verify the excellent sensing ability, those EAAs with single form were analyzed with concentrations from 10 fmol/L to 100 pmol/L. As expected, the experimental results basically agreed with the LOD inferred from the linear equation (Fig. S13 in Supporting information).

The sensing repeatability of EG-OFET was subsequently examined by successively monitoring for ten times with the same EG. The current of 1% PBS solution kept at stable stage during ten cycles. Meanwhile, the reliability of chiral recognizing capacity was also guaranteed by multiple testing 10 nmol/L D-Phe and 10 nmol/L L-Phe in 1% PBS solution (Fig. S14 in Supporting information). The saturation current changes were reproducible to a certain extent, which illustrated that the CD modified EG for Pisomer resolving was stable. Furthermore, the established EG-OFET sensor was proven to be capable of sensing enantiomer pairs with different enantiomeric excesses using Phe and Lys as model analytes (Fig. S15 in Supporting information). A clear ascendant of the measured current change was clearly observed as the percentage of D-Phe, D-Trp, D-Thr (or L-Lys, L-Leu, L-Met) increased, which indicated a differential selective binding affinity of L-form and D-form on the Im^+-MePh-β-CD layer. An excellent linear relationship between the current response and the composition of Phe (or Lys) was achieved. Then, a quantitation analysis of EAAs enantiomers mixtures was performed. The composition of D-Phe was determined as 0.59 (actual value 0.60) for three repeated experiments. Satisfied result was also obtained for Lys (observed value 0.39; actual value 0.40).

To provide guidance for future work, the transduction mechanism of this EG-OFET was discussed in details. The EG-OFET is operated by applying V_{DS} and V_G biases to three electrode contacts (Fig. S16a in Supporting information). Upon application of negative potential (V_0) by a calomel electrode, the ions in electrolytes redistribute so that cations (H^+, Na^+, K^+) face the negatively biased calomel electrode while anions (Cl^-, $HPO_4{}^{2-}$, H_2PO^{4-}, OH^-) align near to the gate surface. Accordingly, V_0 could be applied to semiconductor layer ($V_C = V_0$) and introduce positive holes in initial situation. This conclusion could also be confirmed by replacing PBS buffer by pure water, where no normal output curve was obtained. When Au gate is functionalized by Im^+-MePh-β-CD, the negative potential (V_0) could not efficiently transfer to the channel, as CDs layer needs to be passed. The cationic imidazolium group, whose electropositivity is partially shielded as included in the extended CD cavity [27], just like a "switch" in off-state, would cause a potential dropping ($V_C < V_0$) accompanied by positive holes reduction (Fig. S16b in Supporting information). After combination of chiral analytes, the imidazolium moiety is "squeezed" out of CD cavity and "turned on" more electropositivity, contributing to the further obvious current decrease of EG-OFET platform.

As known from ROSEY spectra (Fig. 2), EAAs do not interact with the cycloskeleton of Im^+-MePh-β-CD but prefer binding with the phenlycarbamoyl moieties. The complexation of AAs occurs in the extended hydrophobic cavity formed by 4-methylphenlycarbamoyl substituents that modified on CD rims (Fig. S16c in Supporting information). Cationic imidazolium plays as a switch to modulate the voltage at EG.

In the initial situation, cationic moiety shows an off-state by shielding in the extended cavity. When captured by selectors, D-Phe, for example, would deeply embed in extended cavity, push imidazolium group out of CD cavity and turn on electropositivity switch. Therefore, the sensing layer shows more positive charge, contributing to the reduction of effective bias voltage introduced at EG terminal. For L-Phe, the degree of "switch on" is smaller in amplitude owning to different complexing modes from D-Phe. Thus, the weaker deshielding effect of L-Phe leads to the relatively smaller current response (Fig. 3d). At the microscopic level of molecular interaction, cationic imidazolium is farther away from the extended cavity in the complex of Im^+-MePh-β-CD and D-Phe compared to L-form inclusion, revealed in ROSEY results (Fig. 2). Consequentially, D-Phe shows more ability to turn electropositivity up by manipulating the imidazolium switch than L-Phe. Compared with Phe enantiomers, Lys shows inversed sensing results (Figs. 4a and e), where the L-form demonstrates stronger interaction than D-form to turn on the cationic imidazolium switch due to the different branching chains. This "contrary interaction phenomenon" is also perfectly verified by the previous circular dichroism spectra, optical rotation analysis and ^1H NMR data. The above results indicated that the as-fabricated CD sensitized EG-OFET not only provides a versatile chiral sensing platform, but also demonstrates great potential for the investigation of steric interactions between chiral molecules.

In this study, a facile and versatile chirality amplification platform based on a cationic supramolecular charge switch extended-gate field effect transistor was successfully fabricated for essential amino acids enantiodiscrimination. Circular dichroism and NMR results reveal the subtle binding difference between Im^+-MePh-β-CD and AAs as well as the different states of imidazole switch. The weak steric intermolecular interactions can be facilely amplified to more significant signal changes based on the modulation

of gate bias by charge switch. The novel sensing platform affords good chiral resolution of six essential amino acids with good concentration dependence, low detection limitation and enantiomeric excesses determination potential. The results convince us that the as-fabricated sensing tool provides a robust sensing perspective for cryptochiral and difficult-to-separate enantiomers and may afford deeper understanding of molecular chirality.

Declaration of competing interest

The authors declare that they have no known competing financial interests or personal relationships that could have appeared to influence the work reported in this paper.

Acknowledgments

This work was financially funded by the National Key R&D Program of China (No. 2019YFC1905500), the National Natural Science Foundation of China (Nos. 21922409, 21976131) and Tianjin Research Program of Application Foundation and Advanced Technology (No. 18JCZDJC37500).

Supplementary materials

Supplementary material associated with this article can be found, in the online version, at doi:10.1016/j.cclet.2021.11.081.

References

[1] G.K. Banerjee, D.O. Ben, F. Tassinari, et al., Science 360 (2018) 1331–1334.
[2] S.S. Upadhyay, N.S. Gadhari, A.K. Srivastava, Biosens. Bioelectron. 165 (2020) 112397.
[3] C. Xie, L. Gu, Q. Wu, et al., Anal. Chem. 93 (2021) 859–867.
[4] J.E. Elsila, J.C. Aponte, D.G. Blackmond, et al., ACS Cent. Sci. 2 (2016) 370–379.
[5] L.T. Kuhn, C.K. Motiram, T.J. Athersuch, T. Parella, T.M. Perez, Angew. Chem. Int. Ed. 59 (2020) 23615–23619.
[6] A.D. Garcia, C. Meinert, H. Sugahara, et al., Life 9 (2019) 29.
[7] J.S. Creamer, M.F. Mora, P.A. Willis, Anal. Chem. 89 (2017) 1329–1337.
[8] D.P. Glavin, A.S. Burton, J.E. Elsila, J.C. Aponte, J.P. Dworkin, Chem. Rev. 120 (2020) 4660–4689.
[9] F. Yu, Y. Chen, H. Jiang, X. Wang, Analyst 145 (2020) 6769–6812.
[10] X. Niu, X. Yang, H. Li, et al., Microchim. Acta 187 (2020) 187–676.
[11] K. Mislow, P. Bickart, Isr. J. Chem. 15 (1976) 1–6.
[12] H. Zhu, Q. Li, Z. Gao, et al., Angew. Chem. Int. Ed. 59 (2020) 10868–10872.
[13] J. Gawronski, J. Grajewski, Org. Lett. 5 (2003) 3301–3303.
[14] S. Alwera, V. Alwera, S. Sehlangia, Biomed. Chromatogr. 34 (2020) e4943.
[15] S. Rocchi, C. Fanali, S. Fanali, Chirality 27 (2015) 767–772.
[16] U. Woiwode, S. Neubauer, W. Lindner, S. Buckenmaier, M. Laemmerhofer, J. Chromatogr. A 1562 (2018) 69–77.
[17] J. Zou, X.W. Lan, G.Q. Zhao, et al., Microchim. Acta 187 (2020) 636.
[18] Q. Bi, S. Dong, Y. Sun, X. Lu, L. Zhao, Anal. Biochem. 508 (2016) 50–57.
[19] L.I. Immohra, H.M. Pein, Sensor. Actuators B: Chem. 253 (2017) 868–878.
[20] J. Zhang, J. Hu, D. Wu, et al., Biol. Macromol. 129 (2019) 786–791.
[21] Q. Wang, X. Lin, D. Guo, et al., RSC Adv. 5 (2015) 94338–94343.
[22] E. Zor, H. Bingol, A. Ramanaviciene, A. Ramanavicius, M. Ersoz, Analyst 140 (2015) 313–321.
[23] N. Wang, A. Yang, Y. Fu, Y. Li, F. Yan, Acc. Chem. Res. 52 (2019) 277–287.
[24] H. Li, W. Shi, J. Song, et al., Chem. Rev. 119 (2019) 3–35.
[25] Y. Sun, Y. Wang, Y. Wu, et al., Anal. Chem. 90 (2018) 9264–9271.
[26] Y. Wu, X. Wang, X. Li, Y. Xiao, Y. Wang, Chin. Chem. Lett. 30 (2019) 99–102.
[27] Y. Wu, Y. Xiao, X. Wang, X. Li, Y. Wang, ACS Sens. 4 (2019) 2009–2017.
[28] X. Li, X. Jin, X. Yao, X. Ma, Y. Wang, J. Chromatogr. A 1467 (2016) 279–287.
[29] M.J. Axley, R. Fairman, J. Yanchunas, et al., Biochemistry 36 (1997) 812–822.
[30] R. Lysek, K. Borsuk, M. Chmielewski, et al., J. Org. Chem. 67 (2002) 1472–1479.
[31] C. Merten, J.F. Reuther, J.D. DeSousa, B.M. Novak, Phys. Chem. Chem. Phys. 16 (2014) 11456–11460.
[32] H. Goto, J. Jwa, K. Nakajima, A. Wang, J. Appl. Polym. Sci. 131 (2014) 547–557.
[33] G.S. Jadhav, P.R. Vavia, T.D. Nandedkar, AAPS Pharm. Sci. Tech. 8 (2007) E61–E70.
[34] X. Yao, H. Zheng, Y. Zhang, et al., Anal. Chem. 88 (2016) 4955–4964.
[35] M. Rezanka, Eur. J. Org. Chem. 32 (2016) 5322–5334.
[36] J. Song, C. Yang, J. Ma, et al., Microchim. Acta 185 (2018) 230.
[37] D. Wu, Y. Kong, Anal. Chem. 91 (2019) 5961–5967.